Lightning Overvoltages Incoming to a Substation: Analysis with Emphasis on the LEMP Impact

Akifumi Yamanaka, Kazuyuki Ishimoto, and Akiyoshi Tatematsu

***Abstract*—Lightning overvoltages incoming to a substation are important for determining insulation levels of electric power equipment. Although electromagnetic transient (EMT) analysis disregarding lightning electromagnetic pulses (LEMPs) has been widely used for insulation coordination studies, several observational and analytical studies indicated the LEMP impact on overvoltages incoming to a substation. In this study, characteristics of these overvoltages are analyzed by the 3D finite-difference time-domain method for solving Maxwell's equations, EMT analysis with LEMP, and that without LEMP. The analyses clarified that LEMP has almost no impact on overvoltages generated by a shielding failure, whereas it has a significant impact on those generated by a strike on the tower top. In the latter case with a negative lightning current, a positive-polarity voltage induced by LEMP arrives at the substation first, and a negative-polarity overvoltage caused by the back-flashover (BFO) intrudes subsequently. Although similar overvoltage peaks are derived at the substation by each method as long as the BFO voltages at the struck tower are similar and surge arresters suppress them, the current peaks causing BFO are much lower for the analysis with LEMP than for that without LEMP. This result calls for further studies of lightning overvoltages at substations considering the LEMP.**

***Keywords*: EMT analysis, FDTD method, LEMP, Lightning overvoltage, Transmission line, Substation.**

I. Introduction

LIGHTNING overvoltages are one of the dominant factors to determine the insulation levels of a substation. Electro-magnetic transient (EMT) analysis [1] has been widely used to investigate lightning overvoltages because their experimental observations are challenging [2]. Several standardized EMT analysis models and procedures have been developed by research communities and international standards [2]–[6]. In recent studies, lightning protection design techniques also based on EMT analysis have been explored [7]–[10].

Although it is difficult to observe lightning overvoltages in real substations, several observations have been performed and presented. For instance, the literature presented observational results of lightning overvoltages at a 77 kV substation [11]–[13], those at a 500 kV switching substation [14], and those at ultra-high-voltage designed and 500 kV transmission lines (TLs), switching stations, and substations [15]. These observational results, especially those reported in refs. [11]–[14], indicated the impact of the lightning electromagnetic pulse (LEMP), which induces voltages in overhead conductors, on lightning overvoltages incoming to a substation. The LEMP impact is missing in standardized EMT analysis models presented in the literature.

Electromagnetic computation methods can analyze a lightning strike on TLs and resultant lightning overvoltages incoming to a substation more accurately than EMT analysis [16]. This is because electromagnetic computation methods solve electromagnetic phenomena directly and hence do not require the transverse electromagnetic assumption required in EMT analysis. The methods can model return stroke current and LEMP emission, the electromagnetic coupling between the LEMP and the overhead conductors, and 3D structures of electric facilities. Experimental results for scale models of TL towers and a substation [17] and observational results of lightning overvoltages incoming to a 77 kV substation [18] were reproduced using the finite-difference time-domain (FDTD) method for solving Maxwell's equation [19], both in the waveform level. Moreover, the difference between lightning overvoltages at a substation computed by EMT analysis and the FDTD method was pointed out [20], [21].

Although it is advantageous from the viewpoint of analysis accuracy, the electromagnetic computation method requires much more computation resources and time than EMT analysis. More recently, the LEMP impact on direct lightning strikes to distribution lines has been clarified [22]–[24], and an LEMP-incorporated EMT analysis method has been developed and validated for distribution and high-voltage TLs [25], [26]. The LEMP-incorporated EMT analysis method can be performed more rapidly than electro-magnetic computation methods with maintained high accuracy.

In this paper, the characteristics of lightning overvoltages incoming to a substation are analyzed and discussed with emphasis on the LEMP impact. A 77 kV substation with five spans of TLs was studied considering a shielding failure (SF) and a strike on the top of a TL tower. The 3D FDTD analysis for solving Maxwell's equations was considered as a reference, and EMT analyses with and without considering the LEMP impact were performed. The comparison of the three methods and discussion on their results clarify the LEMP impact on lightning overvoltages. The results showed that (i) LEMP has a significant impact on the overvoltages especially generated by a lightning strike on the tower top, which can cause back-flashovers (BFOs), and (ii) EMT analysis with the LEMP impact is applicable to the analysis of these overvoltages.

The rest of the paper is organized as follows. In Sect. II, an overview of the analyzed 77 kV system in the beginning and then the details of analysis models employed in the 3D FDTD

A. Yamanaka, K. Ishimoto, and A. Tatematsu are with the Central Research Institute of Electric Power Industry, 2-6-1 Nagasaka, Yokosuka-shi, Kanagawa 240-0196, Japan (e-mail: yamanaka3929@criepi.denken.or.jp; ishimoto@criepi.denken.or.jp; akiyoshi@criepi.denken.or.jp).

Paper submitted to the International Conference on Power Systems Transients (IPST2025) in Guadalajara, Mexico, June 8-12, 2025.

TABLE I
TL TOWER GEOMETRY (UNIT IN METER)

d_1	d_2	d_3	r_1	r_2	r_3	l_s	l_1	l_2	w_1	w_2	w_3
2.5	4.0	2.75	0.25	0.5	3.0	1.0	2.5	0.5	0.5	1.0	1.5

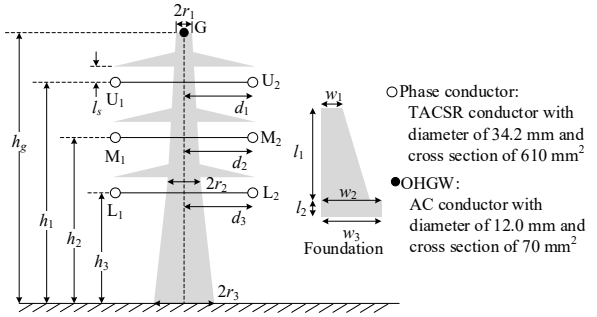

Fig. 1. TL tower geometry and its foundation, and conductor types.

method and EMT analysis are presented. In Sect. III, the analysis results of a SF and a strike on the tower top without and with BFO are presented. In Sect. IV, discussion and concluding remarks are presented. In the Appendix, overvoltages observed in a substation [12] was introduced.

II. ANALYSIS MODELS AND METHODS

A. Specifications of Studied Transmission Line and Substation

A 77 kV TL and a simplified substation model were studied. Table I and Fig. 1 show the conductor types of TLs and the geometry of the tower. Fig. 2 shows the geometry of the substations and incoming lines.

The TL includes five towers and has a span length of 300 m. The substation model consists of a gantry at the entrance, a grounding mesh, buslines, and electrical equipment. In this study, transformers and surge arresters were modeled as the main equipment parts, and other equipment parts, such as disconnecting switches, circuit breakers, potential dividers, and bushings were not modeled for simplicity. The first tower (Tower #1) and the substation entrance were connected by inclined incoming lines. A single overhead grounding wire (OHGW) was employed for the TLs, but as shown in Fig. 2 (b), double OHGWs were employed for the incoming line to prevent direct lightning strikes to the phase conductors (typical arrangement for incoming lines located in the vicinity of a substation).

The lightning impulse withstand voltage of 77 kV systems was assumed as 400 kV. Fig. 3 shows the voltage–time (V–t) curve of the arcing-horn of TLs with a critical flashover voltage of 500 kV [27] as well as the voltage–current (V–I) characteristics of the surge arrester at the substation entrance [6]. The calculated V–t curve shown in Fig. 3(a) was derived using the leader progression model (LPM) employed in the FDTD method and EMT analysis and will be described in detail in the following sections.

B. FDTD Analysis Model for Solving Maxwell's Equations

The 3D FDTD method for solving Maxwell's equations was performed as a reference for this study. As mentioned in Introduction, the FDTD method is suitable for analyzing lightning transients that include 3D electromagnetic phenomena. Several experimental and observational results were reproduced by the FDTD method at the waveform level,

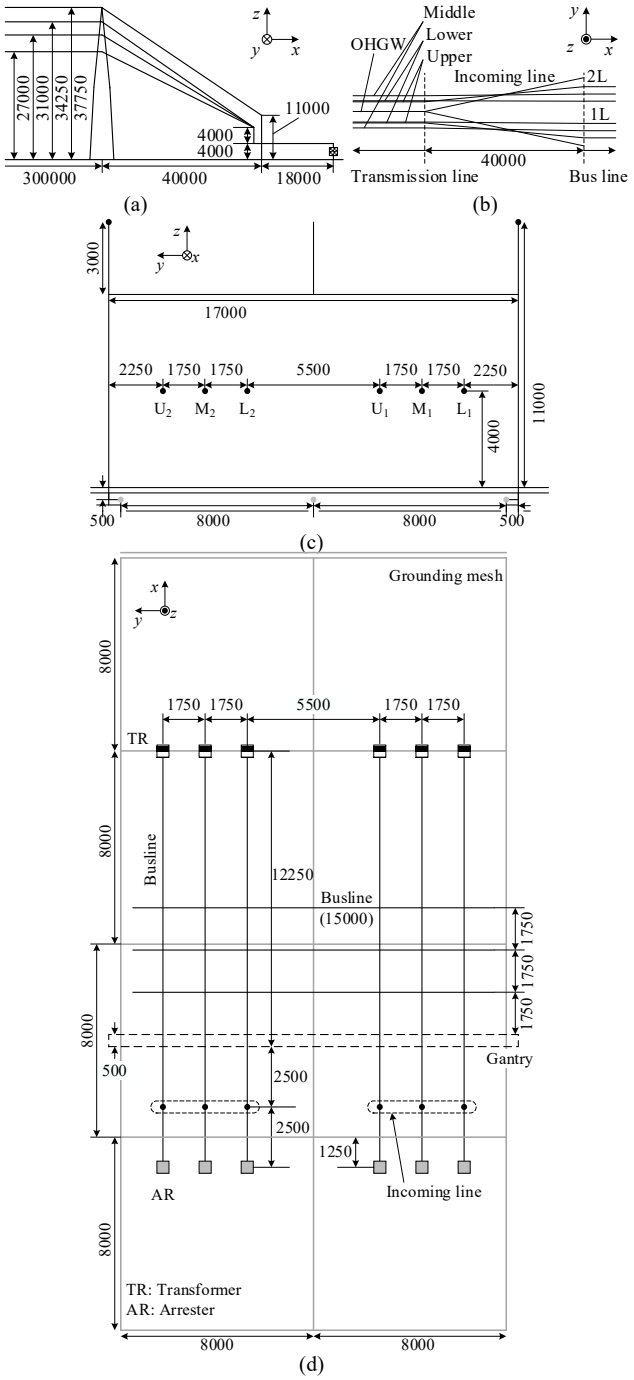

Fig. 2. Geometry of incoming line and substation (unit in millimeter). (a) Side view of the incoming line, (b) top view of the incoming line, (c) the incoming line and gantry at the substation entrance, and (d) top view of the substation.

and the modeling approach adopted in this study follows those reported in literature [17], [18], [20], [21]. The FDTD analysis was performed using Virtual Surge Test Lab. Restructured and Extended Version (VSTL REV) [28].

Fig. 4 shows the entire FDTD analysis space. Five TL towers and a substation were modeled at the center of the analysis space. (i) SF (direct lightning strike to the M_1 phase between Towers #2 and #3) and (ii) a strike on the top of Tower #3 were simulated. The analysis space was divided into non-uniform cells with side lengths of 0.25–10 m, and the total numbers of cells were 1061, 226, and 556 for the x, y, and z directions. The entire analysis space was enclosed by

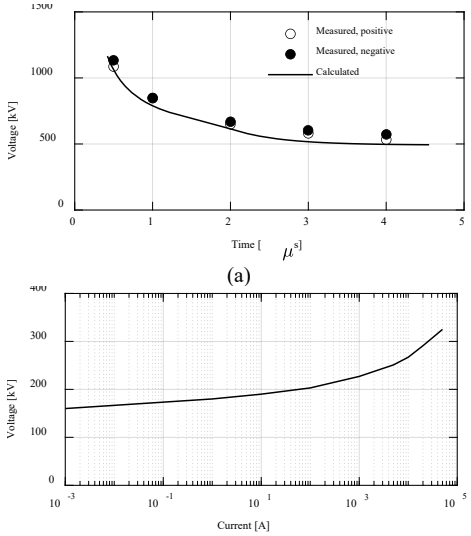

Fig. 3. Characteristics of the studied system. (a) *V–t* curve of the arcing-horn of the TL, and (b) *V–I* characteristics of the surge arrester at the substation entrance.

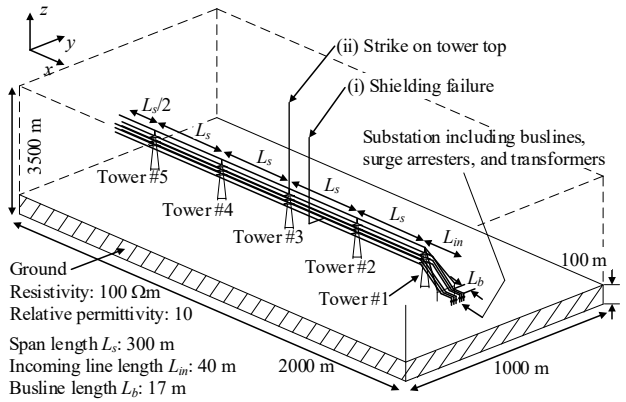

Fig. 4. Analysis space of the FDTD method for solving Maxwell's equations.

Liao's second-order absorbing boundary [29].

The imperfectly conducting ground was modeled in the bottom 100 m of the FDTD analysis space by assuming the constant resistivity of 100 Ωm and relative permittivity of 10. In this study, the frequency dependence of these parameters was disregarded. For example, according to the frequency dependence shown in Fig. 3 of [30], the resistivity decreases to 80 Ωm at 1 MHz for a soil with low-frequency resistivity of 100 Ωm. Thus, in this study, the frequency dependence might have a minor impact on the analysis results, and the constant soil electrical parameters constitute a conservative analysis condition. Nevertheless, the analysis considering the frequency dependence of soil parameters especially with higher soil resistivity is very important to study further.

1) Overhead Line, Incoming Line, and Busline

The single OHGW and the phase conductors with diameters presented in Fig. 1 were modeled by the thin-wire representation method [31]. The inclined incoming lines were modeled by staircase approximation. The sag of the OHGW and phase conductors [32] were not modeled for simplicity. The diameter of the busline was set to be the same as those of the phase conductors. To assume a severe condition (condition for providing a higher overvoltage), the first and second circuits were not connected via the horizontal buslines shown in Fig. 2(d) and the corona wave deformation in the TL was also not considered [2], [6]. The end of the TL on the Tower #5 side was attached to the absorbing boundary.

2) Tower, Tower Footing, and Gantry

The TL towers were modeled in detail including their crossarms, truss structures, tower footing, and foundations. Tower structure was modeled by thin wires (thin wires are represented in the FDTD analysis by forcing the electric field of the corresponding points zero), and the tower foundations were modeled by rectangular conductors considering the geometry shown in Fig. 1 and Table 1. The gantry was modeled by thin wires considering the geometry shown in Fig. 2(c). The width of the gantry was set to 0.5 m (corresponding to the length in *x*-direction shown in Fig. 2 (c)), and 0.5-m long horizontal supporting structures were considered at every 3 m. The legs of the gantry were connected to the grounding mesh of the substation. The tower and gantry models were similar to those shown in Figs. 14 and 15 of ref. [18], where the FDTD analysis results of lightning overvoltages at a 77 kV substation were compared with measured results for validation.

3) Arcing-horn and Substation Equipment

Arcing-horn flashover and substation equipment were modeled using lumped circuit models. The flashover of the arcing-horn with a gap length of 0.65 m was modeled using the LPM [33], and the parameters presented in [18] were employed in this study. The leader onset condition is

$$V > 500 \times D, \tag{1}$$

where V [kV] is the arcing-horn voltage, and D [m] is the gap length. Leader progression process is defined by

$$I_L = 2K_0 v_L, \tag{2}$$

$$v_L = \begin{cases} K_1'\left(\dfrac{V}{D-2X_L} - E_0\right) & \left(0 \le X_L \le D/4\right) \\ K_1''\left(\dfrac{V}{D-2X_L} - E_0'\right) + v_L' & \left(D/4 < X_L \le D/2\right) \end{cases}, \tag{3}$$

$$X_L = \int v_L dt, \tag{4}$$

where I_L [A], v_L [m/s], and X_L [m] are the leader current, leader progression speed, and average leader length (the average of the upper and lower leaders), respectively. The constants were defined on the basis of the measurement [33] and the *V–t* curve shown in Fig. 3 (a): K_0 = 410 [μC/m], K'_1 = 0.70 [m^2/Vs], K''_1 = 0.42 [m^2/Vs], E_0 = 750 [kV/m]. E'_0 and v'_L in (3) are the values of $V/(D-2X_L)$ and v_L, respectively, immediately before X_L exceeds $D/4$. Break down is judged by

$$X_L > D/2. \tag{5}$$

Criterion to stop the process of leader progression is

$$\frac{V}{D-2X_L} < E_0. \tag{6}$$

The transformers were modeled by a capacitance of 1000 pF [6]. The surge arresters at the substation entrance were modeled by the nonlinear resistor with the *V–I* characteristics shown in Fig. 3(b); the frequency-dependent model [34] was not employed in this study [6].

4) Lightning Channel and Source Model

The lightning channel was modeled using the TL model [35] with a return stroke speed of 100 m/μs. The lightning

channel was assumed to be vertical and straight for (ii) a strike on the tower top. For (i) SF, the bent point was set to 30 m from the struck point (this length corresponds to the striking distance of 10 kA lightning current according to an electro-geometric model); the channel above the bent point was set to be vertical and straight, and the channel from the bent point to the struck point (M_1 phase conductor) was set to be horizontal and straight.

The lightning channel impedance was infinity because of the use of the TL model. Although the use of a finite lightning channel impedance is preferred, in this study, the TL model was adopted to inject the same lightning current, to consider the same channel impedance, and to consider the same temporal and spatial distribution of the current along the channel between the FDTD method and the EMT analysis. This aspect was discussed in detail in [26].

A lightning current waveform with the median parameters of observational results in TLs in Japan [36] for its wavefront characteristics—a current peak of 29.3 kA, a rise time of 3.2 μs, and a maximum steepness of 18.3 kA/μs—was used in this study. The current waveform was synthesized using the CIGRE function [37] as shown in Fig. 5.

C. EMT Analysis Models

EMT analysis was performed with and without considering the LEMP impact. The models employed in each case were basically the same, but the tower model was different following ref. [26]. Each model is described in this section.

1) Overhead Line, Incoming Line, and Busline

The overhead lines and buslines were modeled by Agrawal et al. field-to-line coupling formula [38]. The formula for the multiconductor overhead line with the length l in the frequency domain can be written as follows [39].

$$V_0 - Z_c I_0 = \exp(-\Gamma l)(V_l + Z_c I_l) + U_0, \quad (7a)$$

$$V_l - Z_c I_l = \exp(-\Gamma l)(V_0 + Z_c I_0) + U_l, \quad (7b)$$

where V_0 and V_l are the voltages, and I_0 and I_l are the currents at both ends of the line, Z_c is the characteristic impedance, Γ is the propagation constant, and U_0 and U_l are voltage sources for considering the effects of the incident electric fields as provided by

$$U_0 = -\int_0^l \exp(-\Gamma x) E_h(x)\, dx - V_0^i + \exp(-\Gamma l) V_l^i, \quad (8a)$$

$$U_l = \int_0^l \exp\left[-\Gamma(l-x)\right] E_h(x)\, dx - V_l^i + \exp(-\Gamma l) V_0^i, \quad (8b)$$

where x is the distance from the left end of the line to the calculation point, E_h is the incident horizontal electric field in the absence of the overhead lines, and V_0^i and V_l^i are the incident voltages

$$V_0^i = -\int_0^h E_v(0,z)\, dz, \quad (9a)$$

$$V_l^i = -\int_0^h E_v(l,z)\, dz, \quad (9b)$$

where h is the height of the line, z is the height from the ground, and E_v is the incident vertical electric field.

In this study, (7) was rewritten as follows to consider the Norton equivalent [40]:

$$I_0 = Y_c V_0 - \exp(-\Gamma l)^T (Y_c V_l + I_l) - Y_c U_0, \quad (10a)$$

$$I_l = Y_c V_l - \exp(-\Gamma l)^T (Y_c V_0 + I_0) - Y_c U_l, \quad (10b)$$

where Y_c is the characteristic admittance and T denotes the matrix transposition. In the EMT analysis, (10) was solved in the time domain [40]. The effects of the incident electric fields, U_0 and U_l shown in (8), were solved in the phase domain using composite Simpson's rule as proposed in [41].

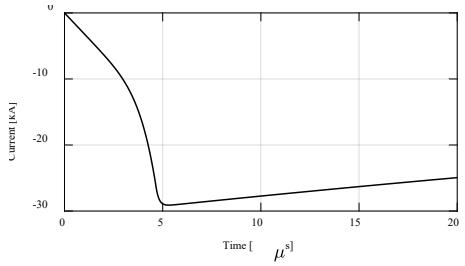

Fig. 5. Lightning current waveform employed for the analysis.

The inclined incoming line was modeled by staircase approximation in Agrawal et al. formula. The incoming line with a horizontal length of 40 m, as shown in Fig. 2(a) and (b), was divided into 10, and the line constants of each section were calculated on the basis of the impedance and admittance formula for finite-length conductors [42].

The effects of incident electric fields, U_0 and U_l shown in (8), were considered for the EMT analysis with the LEMP, whereas they were not considered (set to zero) for the EMT analysis without the LEMP. The end of the TL on the Tower #5 side was grounded via a multiphase matching circuit.

2) Tower, Tower Footing, and Gantry

For the EMT analysis without the LEMP impact, the tower was modeled using the multistory tower model with dumping *RL* parallel circuits [43], as one of the most representative tower models adopted in a lot of literature [2], [5], [6], [8], [9]. Note that the multistory tower model was optimized so that the experimental result obtained for a 500 kV tower can be accurately reproduced by the EMT analysis without considering the LEMP effect [43].

For the EMT analysis with the LEMP, the TL tower was modeled using cascade-connected lossless distributed lines. In [26], this simple model was examined for EMT analysis with the LEMP because other sophisticated tower models such as the multistory tower model were optimized for EMT analysis without LEMP. Then, it was shown that this simple model can provide sufficiently accurate arcing-horn voltages in comparison with the results obtained by the FDTD analysis for solving Maxwell's equations. Further discussion was presented in [26]. The surge impedance was calculated using modified Jordan's formula [44]: 208 Ω for the studied tower.

The tower footing was modeled using a lumped resistance. The soil resistivity was set to 100 Ωm, and the tower footing resistance was calculated to be 3.5 Ω [26]. It was confirmed from the FDTD analysis that the studied tower footing with the soil resistivity of 100 Ωm can be modeled by the lumped resistance model with satisfactory accuracy: the footing has little frequency dependence. Note that for higher soil resistivity conditions, larger foundations, or foundations with counterpoise wires, it is better to represent the tower footing using the frequency-dependent model presented in, e.g, [45].

The gantry was modeled using a single lossless distributed parameter line with a surge impedance of 100 Ω and a current traveling speed of 210 m/μs [6]. The grounding resistance of

the gantry was set to 1.0 Ω. The grounding mesh was not considered explicitly in the EMT analysis, and it was regarded as a zero-potential surface [2].

3) Arcing-horn and Substation Equipment

The same models for arcing-horn flashovers, transformers, and surge arresters as those employed in the FDTD analysis presented in Sect. III.B.3 were used in the EMT analysis.

4) Lightning Channel and Source Models

The lightning source was modeled using the current source in parallel with the channel impedance. As described in Section III.B.4, the lightning channel impedance was set to infinity in this study.

For the EMT analysis considering the LEMP impact, the lightning channel was considered to derive the incident electric field to overhead conductors. The current distribution along the channel was determined using the TL model, and the electric field from the channel was calculated using retarded potential formulae [25]. The lightning channel bent for (i) SF analysis was represented by the superimposition of the formulae as presented in [46].

III. Analysis Results

To clarify the LEMP impact on lightning overvoltages, the following three analyses were performed:

(i) SF analysis with normalized current not causing flashover

(ii-1) analysis for the strike on the tower top with normalized current not causing BFO.

(ii-2) analysis for the strike on the tower top with lightning current causing BFO considering AC operating voltages.

It will be shown that the LEMP has almost no impact on the overvoltages generated by the SF, whereas it has a significant impact on the overvoltages generated by a strike on the tower top (thus, two cases of the analysis for the strike on the tower top were performed).

A. Shielding Failure

SF analysis (lightning strike on the M_1 phase between Towers #2 and #3 as shown in Fig. 4) was performed with the normalized lightning current waveform. Fig. 6 shows the arcing-horn voltage of the M_1 phase at Tower #3 and the voltage rise of the surge arrester at the substation entrance. In the figure, the results of the EMT analysis with and without considering the LEMP impact are shown as "EMT-with-LEMP" and "EMT-without-LEMP," respectively, and those derived by the FDTD method are shown as "FDTD."

One can find that the LEMP has almost no impact on the voltages generated by the SF: the three analysis methods provide almost the same results. For the SF, the voltage rise of the phase conductor, obtained from the product of the lightning current $i(t)$ and the surge impedance of the stuck line Z_c, $v(t) = (Z_c/2)\times i(t)$, predominantly determines the voltages of the arcing-horn and surge arrester in the wavefront. Then, the boundary condition of TL changes the voltage waveform: in the present case, the voltage was doubled because the TL was open-circuited via the capacitance of 1000 pF representing the transformer on the substation side, and the matching condition

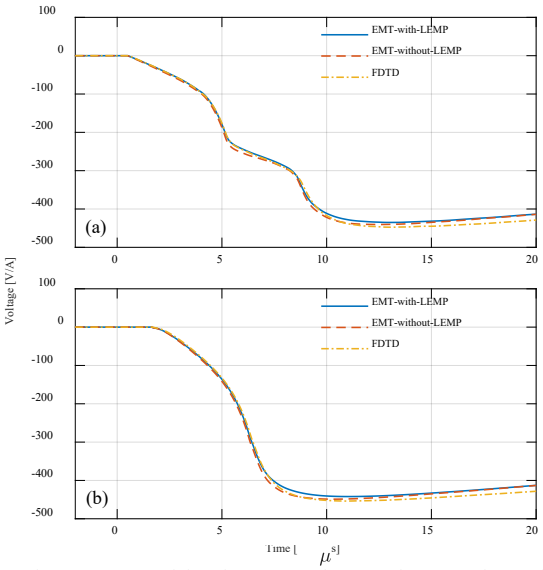

Fig. 6. Voltages generated by the SF on the M_1 phase conductor between Towers #2 and #3; the current peak was normalized to 1 A. (a) M_1 phase arcing-horn voltage of Tower #3 and (b) voltage of the M_1 phase surge arrester at the substation. The arcing-horn voltage was defined from the tower side to the phase conductor side.

(no reflection of traveling wave) was adopted on the other side (Tower #5 side). The voltages induced by the LEMP are on the order of 10 V/A, as shown in Fig. 7(b), and hence, LEMP has almost no impact on the voltages generated by the SF.

B. Strike on Tower Top—Normalized Current without BFO

The lightning strike on the top of Tower #3 was analyzed with normalized lightning current to clarify the characteristics of lightning overvoltages incoming to a substation without considering the effect of the BFO at the struck tower and the operation of the surge arrester at the substation entrance.

The LEMP has a significant impact on the voltages generated by a strike on the tower top as follows. Fig. 7 shows the U_1 phase arcing-horn voltage of Tower #3 and the voltage of the U_1 phase surge arrester at the substation. The arcing-horn voltage determined by the EMT analysis without the LEMP is much lower than those determined by the EMT analysis with the LEMP and the FDTD method. This result was obtained because the LEMP induces voltages with a polarity opposite to those generated by the lightning current flowing into the tower and the OHGW [11]–[14], [17], [18], [20]–[26]. Furthermore, as shown in Fig. 7(b), the EMT analysis without the LEMP provided an almost zero voltage rise for the U_1 phase surge arrester at the substation entrance, whereas the EMT analysis with the LEMP and the FDTD method provided a positive-polarity voltage rise. The results clearly show that the LEMP significantly affects the voltages generated by the lightning strike on the tower top. Note that Fig. A1(a) shows the observed voltage reported in [12].

The characteristics of the voltage of the surge arrester at the substation are further described with a conceptual sketch shown in Fig. 8. The voltage rise obtained by the EMT analysis without the LEMP was almost zero. This is because the OHGW voltage drops owing to grounding via the TL towers and gantry while it travels toward the substation, and the phase conductor voltage predominantly determined by the

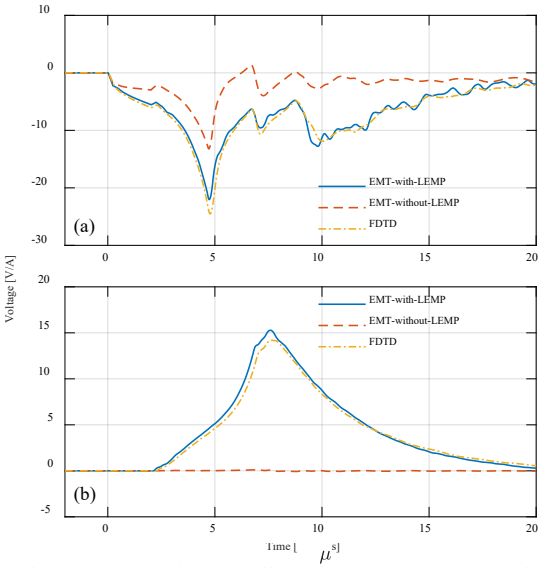

Fig. 7. Voltages generated by the strike on the top of Tower #3; the current peak was normalized to 1 A. (a) U_1 phase arcing-horn voltage of Tower#3, and (b) voltage of the U_1 phase surge arrester at the substation. The arcing-horn voltage was defined from the phase conductor side to the tower side.

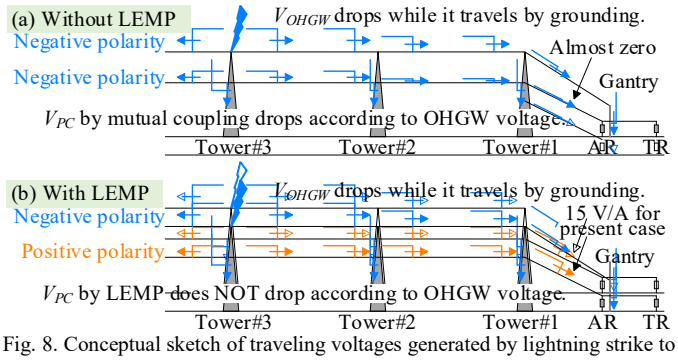

Fig. 8. Conceptual sketch of traveling voltages generated by lightning strike to tower top (a) without LEMP effect and (b) with LEMP effect. V_{OHGW} denotes the OHGW voltage, and V_{PC} denotes the phase conductor voltage.

mutual coupling from the OHGW drops in accordance with the OHGW voltage. In general, the grounding resistance of towers near the substation and that of gantry are maintained to be low (3.5 and 1.0 Ω were adopted in the EMT analysis in this study assuming a soil resistivity of 100 Ωm). In contrast, the voltage rise obtained by the EMT analysis with the LEMP and the FDTD method exhibits a peak of about 15 V/A with positive polarity. This voltage is induced by the LEMP not greatly affected by the grounding via the tower and gantry as in the case of the traveling voltage of the OHGW. Thus, the LEMP impact results in the markedly different characteristics of the voltages generated by the strike on the tower top.

C. Strike on Tower Top—Lightning Current with BFO

The lightning strike on the top of Tower #3 was analyzed with the BFO occurrence considered. In this analysis, AC operating voltages were considered. The voltage sources were inserted into the Tower #5 side of the line, and the phase conductors were energized so that the upper phase held the highest positive AC voltage. The LPM was inserted in the U_1 phase. Moreover, to evaluate the lightning overvoltages incoming to the substation under a similar condition resulting from the BFO at the struck tower with similar voltage and timing, different current peaks were adopted for each analysis

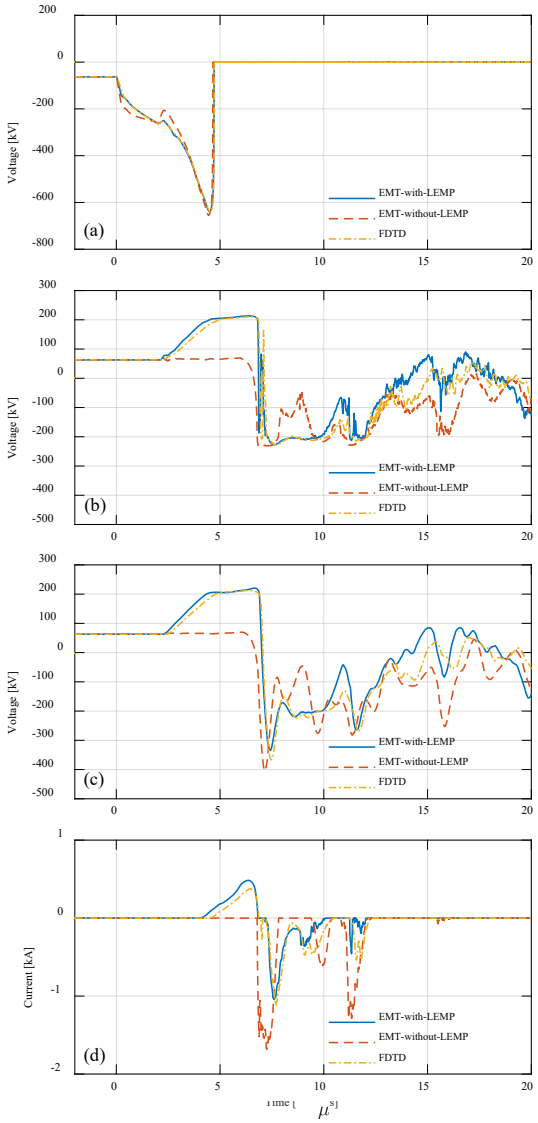

Fig. 9. (a)–(c) Overvoltages and (d) current generated by the lightning strike on the top of Tower #3 with BFO. (a) voltage of the U_1 phase arcing-horn of Tower #3, (b) voltage of the U_1 phase surge arrester at the substation entrance, (c) voltage of the U_1 phase at the transformer, and (d) current flowing through the U_1 phase surge arrester at the substation entrance. The arcing-horn voltage was defined from the phase conductor side to the tower side.

method as follows: (a) 38 kA for the EMT analysis with the LEMP, (b) 66 kA for that without the LEMP, and (c) 35 kA for the FDTD method. These current peaks were roughly determined from the scaling of the voltage peaks obtained using the normalized current shown in Fig. 7 initially, and then the peaks were fixed through a try-and-error method so that very similar BFO waveforms can be obtained by each method. As shown in Fig. 9(a), the BFO occurs with almost the same voltage and timing in each method. Note that the current rise time was not changed from the waveform shown in Fig. 5, but the current peak was changed to each value.

The LEMP has a significant impact on the characteristics of the overvoltages generated by the strike on the tower top associated with the BFO as follows. The results derived by the EMT analysis with the LEMP and the FDTD method depicted in Fig. 9(b) and (c) show that the positive-polarity overvoltage induced by the LEMP arrives at the substation first, and the surge arrester at the substation entrance even operates to

suppress the overvoltage ((b) the surge arrester voltage is suppressed within about 200 kV and (d) the positive surge arrester current flows). After several microseconds corresponding to the sum of the wave traveling time from Tower#3 to the substation and the time until the BFO occurs, the negative-polarity overvoltage associated with the BFO arrives at the substation. This overvoltage generates the highest peak voltage to the transformer (Fig. 9(c)) because it includes the abrupt voltage change due to the BFO. The results derived by the EMT analysis without the LEMP do not exhibit the positive-polarity overvoltage, and the negative-polarity overvoltage associated with the BFO just arrives at the substation and generates the highest peak voltage to the transformer. The LEMP impact generates significantly different overvoltage waveforms. Fig. A1(b) shows the observed voltage reported in [12].

Note that, although waveform characteristics are different between analyses with and without the LEMP impact (EMT analysis with the LEMP and FDTD method vs EMT analysis without the LEMP), the peaks of transformer voltage are almost the same under the conditions of this study. This is because the surge arrester at the substation entrance effectively suppresses the overvoltage associated with the BFO (even the voltage peaks derived with the LEMP impact considered are lower owing to the positive-polarity-induced voltage). Note that the energy stressing the surge arrester was 362, 513, and 400 J for EMT analysis with LEMP, that without LEMP, and the FDTD analysis, respectively.

IV. Discussion and Concluding Remarks

The results of this study show that the LEMP has a significant impact on the characteristics of voltage waveforms incoming to a substation entrance for a lightning strike on the tower top (or midspan of OHGWs). The positive-polarity-induced voltage generated by the LEMP (assuming a negative return stroke) arrives at the substation firstly, and the negative-polarity overvoltage intrudes subsequently if the BFO occurs at the struck tower. These results reconfirmed the findings of previous studies [11]–[14], [17], [18], [20], [21]. The LEMP has almost no effect on the voltages generated by the SF because the lightning current flowing into the struck conductor predominantly determines the voltage rises.

The positive-polarity-induced voltage generated by the LEMP is discussed from the viewpoint of the insulation coordination. In the event without BFO, this positive voltage would not have a critical impact because a substation and its equipment are designed to withstand the voltages due to the BFO that are higher than the positive voltage. Note that the same phase-to-ground voltages are induced by the LEMP for three phase conductors, whereas the BFO at a single phase is generally assumed in an insulation coordination design. Thus, the effect of positive induced voltage by the LEMP is still important to study further from the insulation coordination viewpoint. In the event with BFO, according to Fig. 9(c), the negative voltage peaks obtained by the FDTD method and the EMT analysis with LEMP are lower than that obtained by the EMT analysis without LEMP owing to the positive induced voltage by the LEMP. This result implies the possibility of reducing the withstand voltage of substation equipment, which results in cost reduction. On the other hand, phase-to-phase voltages can become higher due to the induced voltage by the LEMP when the BFO occurs at a single phase. Thus, the LEMP effect in the event with BFO is also important to study further from the insulation coordination viewpoint.

In this study, different lightning current peaks were adopted for analyzing the event with the BFO to derive similar BFO voltages at the struck tower. In the analysis, similar current peaks were adopted for the EMT analysis with the LEMP and the FDTD method, namely, 38 kA and 35 kA, respectively, but a much higher peak current of 66 kA was adopted for the EMT analysis without the LEMP. It was confirmed that by giving a similar BFO voltage at the struck tower, similar peaks of lightning overvoltage at the transformer with or without LEMP consideration can be obtained as long as the surge arresters effectively suppress the overvoltage incoming to the substation. However, rather higher lightning overvoltages can be generated at transformers if the higher current peak is adopted for the EMT analysis with the LEMP and the FDTD method; this issue also requires further studies on lightning overvoltages incoming to a substation considering the LEMP effect. This study showed the applicability of EMT analysis with the LEMP impact to analyze lightning overvoltages at substations: hence, statistical analysis of lightning overvoltages considering various influencing factors will be performed using the EMT analysis with the LEMP.

V. References

[1] H. Dommel, “Digital computer solution of electromagnetic transients in single-and multiphase networks,” *IEEE Trans. Power Apparat. Syst*., vol. PAS-88, no. 4, pp. 388–399, Apr. 1969.

[2] A. Ametani and T. Kawamura, “A method of a lightning surge analysis recommended in Japan using EMTP,” *IEEE Trans. Power Del.*, vol. 20, no. 2, pp. 867–875, Apr. 2005.

[3] IEEE Modelling and Analysis of System Transients Working Group, “Modeling guidelines for fast front transients,” *IEEE Trans. Power Del.*, vol. 11, no. 1, pp. 493–506, Jan. 1996.

[4] A. R. Hileman, Insulation coordination for power systems, CRC Press, Boca Raton, FL, 1999.

[5] IEC/TR 60071-4 Insulation co-ordination – Part4: Computational guide to insulation co-ordination and modelling of electrical networks, 2004.

[6] Subcommittee for power stations and substations, study committee on lightning risk, “Guide to lightning protection design of power stations, substations, and underground transmission lines (rev. 2021),” *CRIEPI Rep.*, no. H20014, Feb. 2022. (in Japanese)

[7] M. S. Savic and A. M. Savic, “Substation lightning performance estimation due to strikes into connected overhead lines,” *IEEE Trans. Power Del.*, vol. 30, no. 4, pp. 1752–1760, Aug. 2015.

[8] S. Bedoui and A. Bayadi, “Probabilistic evaluation of the substation performance under incoming lightning surges,” *Electr. Power Syst. Res.*, vol. 162, pp. 125–133, Sep. 2018.

[9] Y. Wang, J. Jiang, and Y. Huang, “Lightning fault assessment and protection design of substation in CFETR,” *IEEE Trans. Plasma Sci.*, vol. 52, no. 9, pp. 3412–3417, Sep. 2024.

[10] F. Safaei and M. Niasati, “A new method for surge arrester placement in high-voltage substations considering environmental effects,” *IET Sci. Meas. Technol.*, vol. 18, no. 9, pp. 550–563, Nov. 2024.

[11] S. Kojima, M. Kan, S. Yokoyama, and T. Ueda, “Evaluation of backflashover taking induced voltages by return stroke current into considerations,” *IEEJ Trans. Power Energy*, vol. 113, no. 11, pp. 1249–1255, Nov. 1993. (in Japanese)

[12] T. Ueda et al. “Measurement of lightning surges into 77 kV substations,” *IEEJ Trans. Power Energy*, vol. 114, no. 1, pp. 45–52, 1994. (in

Japanese)
[13] T. Ueda, M. Yoda, and I. Miyachi, "Characteristics of lightning surges observed at 77 kV substations," *IEEJ Trans. Power Energy*, vol. 116, no. 11, pp. 1422–1428, Nov. 1996. (in Japanese)
[14] T. Sonoda, H. Morii, and S. Sekioka, "Observation of lightning overvoltage in a 500 kV switching station," *IEEE Trans. Power Del.*, vol. 32, no. 4, pp. 1828–1834, Aug. 2017.
[15] S. Okabe, T. Tsuboi, and J. Takami, "Analysis of aspects of lightning strokes to large-sized transmission lines," *IEEE Trans. Dielect. Electr. Insul.*, vol. 18, no. 1, pp. 182–191, Feb. 2011.
[16] CIGRE WG C4.37, "Electromagnetic computation methods for lightning surge studies with emphasis on the FDTD method," *CIGRE Technical Brochure*, no. 785, Dec. 2019.
[17] J. Takami et al., "Lightning surge response of a double-circuit transmission tower with incoming lines to a substation through FDTD simulation," *IEEE Trans. Dielect. Electr. Insul.*, vol. 21, no. 1, pp. 96–104, Feb. 2014.
[18] A. Tatematsu and T. Ueda, "FDTD-based lightning surge simulation of an HV air-insulated substation with back-flashover phenomena," *IEEE Trans. Electromagn. Compat.*, vol. 58, no. 5, pp. 1549–1560, Oct. 2016.
[19] K. Yee, "Numerical solution of initial boundary value problems involving Maxwell's equations in isotropic media," *IEEE Trans. Antennas Propagat.*, vol. 14, no. 3, pp. 302–307, May 1966.
[20] J. Takami et al., "Lightning surge into a substation at a back-flashover and review of lightning protective level through the FDTD simulation," *IEEE Trans. Dielect. Electr. Insul.*, vol. 21, no. 3, pp. 1044–1052, Jun. 2014.
[21] J. Takami, T. Tsuboi, K. Yamamoto, S. Okabe, and Y. Baba, "FDTD simulation considering an AC operating voltage for air-insulation substation in terms of lightning protective level," *IEEE Trans. Dielect. Electr. Insul.*, vol. 22, no. 2, pp. 806–814, Apr. 2015.
[22] A. Borghetti, K. Ishimoto, F. Napolitano, C. A. Nucci, and F. Tossani, "Assessment of the effects of the electromagnetic pulse on the response of overhead distribution lines to direct lightning strikes," *IEEE Open Access J. Power Energy*, vol. 8, pp. 522–531, 2021.
[23] K. Ishimoto, F. Tossani, F. Napolitano, A. Borghetti, and C. A. Nucci, "Direct lightning performance of distribution lines with shield wire considering LEMP effect," *IEEE Trans. Power Del.*, vol. 37, no. 1, pp. 76–84, Feb. 2022.
[24] K. Ishimoto, F. Tossani, F. Napolitano, A. Borghetti, and C. A. Nucci, "LEMP and ground conductivity impact on the direct lightning performance of a medium-voltage line," *Electr. Power Syst. Res.*, vol. 214, no. 108845, Jan. 2023.
[25] A. Yamanaka, K. Ishimoto, and A. Tatematsu, "Direct lightning surge analysis of distribution lines considering LEMPs from lightning channel and struck pole in EMT simulation," *IEEE Trans. Electromagn. Compat.*, vol. 65, no. 6, pp. 1909–1920, Dec. 2023.
[26] A. Yamanaka, K. Ishimoto, and A. Tatematsu, "Incorporating the LEMP impact on lightning surge analysis of transmission lines in EMT simulators," *IEEE Trans. Power Del.*, vol. 39, no. 3, pp. 1918–1930, Jun. 2024.
[27] *Electrical Engineering Handbook*, Inst. Electr. Eng. Jpn., Tokyo, Japan, 1978. (in Japanese)
[28] A. Tatematsu, "Development of a surge simulation code VSTL REV based on the 3D FDTD method," *in 2015 IEEE Intl. Sym. Electromagn. Compat. (EMC)*, Aug. 2015, pp. 1111–1116.
[29] Z. P. Liao, H. L. Wong, B. P. Yang, and Y. F. Yuan, "A transmitting boundary for transient wave analysis," *Scientia Sinica*, vol. A27, no. 10, pp. 1063–1076, Oct. 1984.
[30] R. Alipio and S. Visacro, "Frequency dependence of soil parameters: effect on the lightning response of grounding electrodes," *IEEE Trans. Electromagn. Compat.*, vol. 55, no. 1, pp. 132–139, 2013.
[31] T. Noda and S. Yokoyama, "Thin wire representation in finite difference time domain surge simulation," *IEEE Trans. Power Del.*, vol. 17, no. 3, pp. 840–847, Jul. 2002.
[32] E. Stracqualursi, R. Araneo, N. Ravichandran, A. Andreotti, and S. Celozzi, "Modeling of conductors catenary in power lines: effects on the surge propagation due to direct and indirect lightning," *IEEE Trans. Electromagn. Compat.*, vol. 65, no. 5, pp. 1464–1475, Oct. 2023.
[33] H. Motoyama, "Experimental study and analysis of breakdown characteristics of long air gaps with short tail lightning impulse," *IEEE Trans. Power Del.*, vol. 11, no. 2, pp. 972–979, Apr. 1996
[34] IEEE WG 3.4.11, "Modeling of metal oxide surge arresters," *IEEE Trans. Power Del.*, vol. 7, no. 1, pp. 302–309, Jan. 1992.
[35] Y. Baba and V. A. Rakov, "On the transmission line model for lightning return stroke representation," *Geophys. Res. Lett.*, vol. 30, no. 24, Dec. 2003.
[36] J. Takami and S. Okabe, "Observational results of lightning current on transmission towers," *IEEE Trans. Power Del.*, vol. 22, no. 1, pp. 547–556, Jan. 2007.
[37] CIGRE SC 33 WG 01, "Guide to procedures for estimating the lightning performance of transmission lines," *CIGRE Technical Brochure*, no. 63, Oct. 1991 (republished in Jun. 2021).
[38] A. K. Agrawal, H. J. Price, and S. H. Gurbaxani, "Transient response of multiconductor transmission lines excited by a nonuniform electromagnetic field," *IEEE Trans. Electromagn. Compat.*, vol. EMC-22, no. 2, pp. 119–129, May 1980.
[39] C. R. Paul, Analysis of multiconductor transmission lines, 2nd Ed., John Wiley & Sons. Inc., Hoboken, NJ, 2007.
[40] A. Yamanaka, and K. Ishimoto, "Application of integral-based solution of field-to-line coupling formula to direct lightning surge analysis of distribution lines," *IEEJ Trans. Electr. Electron. Eng., in press.*
[41] A. De Conti and O. E. S. Leal, "Time-domain procedures for lightning-induced voltage calculation in electromagnetic transient simulators," *IEEE Trans. Power Del.*, vol. 36, no. 1, pp. 397–405, Feb. 2021.
[42] A. Ametani, N. Nagaoka. Y. Baba. T. Ohno, and L. Yamabuki, Power systems transients, theory and applications, CRC Press, Boca Raton, FL, 2017.
[43] M. Ishii et al., "Multistory transmission tower model for lightning surge analysis," *IEEE Trans. Power Del.*, vol. 6, no. 3, pp. 1327–1335, Jul. 1991.
[44] A. De Conti, S. Visacro, A. Soares, and M. A. O. Schroeder, "Revision, extension, and validation of Jordan's formula to calculate the surge impedance of vertical conductors," *IEEE Trans. Electromagn. Compat.*, vol. 48, no. 3, pp. 530–536, Aug. 2006.
[45] R. Alipio, A. De Conti, F. Vasconcellos, F. Moreira, N. Duarte, and J. Martí, "Tower-foot grounding model for EMT programs based on transmission line theory and Marti's model," *Electr. Power Syst. Res.*, vol. 223, no. 109584, 2023.
[46] A. Yamanaka, K. Ishimoto, and A. Tatematsu, "Inclined and tortuous lightning channel impact on lightning performance assessment of distribution lines with a shield wire," *in Proc. 2024 37th Intl. Conf. Lightning Protection*, Dresden, Germany, no. 36, Sep. 2024.

VI. APPENDIX

Fig. A1 shows the overvoltage waveforms obtained at an entrance of a 77 kV substation [12]. The positive induced voltage by the LEMP was observed in the event without the BFO (Fig. A1(a)), and the positive induced voltage followed by the negative overvoltage suppressed by the surge arresters was observed in the event with the BFO (Fig. A1(b)).

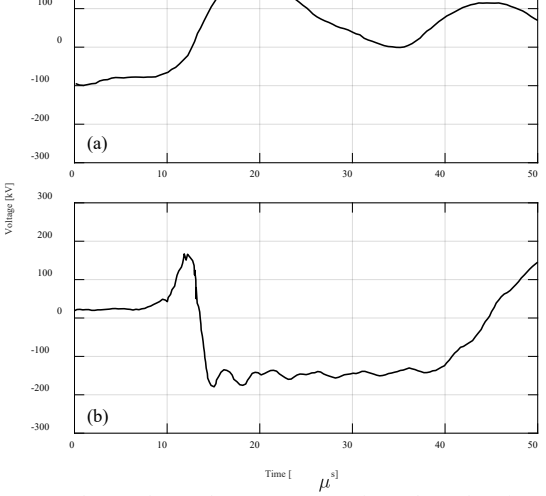

Fig. A1. Overvoltages observed at an entrance of a 77 kV substation [12]. (a) Overvoltage observed without the BFO adapted from Fig. 8 of [12], and (b) that observed with the BFO adapted from Fig. 6 of [12].